Entropy **2014**, *16*, 2530-2548; doi:10.3390/e16052530

OPEN ACCESS

entropy

ISSN 1099-4300

www.mdpi.com/journal/entropy

Article

Measuring Instantaneous and Spectral Information Entropies by Shannon Entropy of Choi-Williams Distribution in the Context of Electroencephalography

Umberto Melia [1,*], Francesc Claria [2], Montserrat Vallverdu [1] and Pere Caminal [1]

[1] Department ESAII, Centre for Biomedical Engineering Research, Universitat Politècnica de Catalunya, CIBER of Bioengineering, Biomaterials and Nanomedicine (CIBER-BBN), Barcelona 08028, Spain; E-Mails: montserrat.vallverdu@upc.edu (M.V.); pere.caminal@upc.edu (P.C.)

[2] Department IIE, Lleida University, LLeida, 25003 Spain; E-Mail: claria@diei.udl.es

* Author to whom correspondence should be addressed; E-Mail: umberto.melia@upc.edu; Tel.: +349-3401-7160; Fax: +349-3401-7045.

Received: 6 December 2013; in revised form: 30 April 2014 / Accepted: 5 May 2014 / Published: 9 May 2014

Abstract: The theory of Shannon entropy was applied to the Choi-Williams time-frequency distribution (CWD) of time series in order to extract entropy information in both time and frequency domains. In this way, four novel indexes were defined: (1) partial instantaneous entropy, calculated as the entropy of the CWD with respect to time by using the probability mass function at each time instant taken independently; (2) partial spectral information entropy, calculated as the entropy of the CWD with respect to frequency by using the probability mass function of each frequency value taken independently; (3) complete instantaneous entropy, calculated as the entropy of the CWD with respect to time by using the probability mass function of the entire CWD; (4) complete spectral information entropy, calculated as the entropy of the CWD with respect to frequency by using the probability mass function of the entire CWD. These indexes were tested on synthetic time series with different behavior (periodic, chaotic and random) and on a dataset of electroencephalographic (EEG) signals recorded in different states (eyes-open, eyes-closed, ictal and non-ictal activity). The results have shown that the values of these indexes tend to decrease, with different proportion, when the behavior of the synthetic signals evolved from chaos or randomness to periodicity. Statistical differences (p-value < 0.0005) were found between values of these measures comparing eyes-open and eyes-closed states and between ictal and non-ictal states in the traditional EEG frequency bands. Finally, this paper has demonstrated

that the proposed measures can be useful tools to quantify the different periodic, chaotic and random components in EEG signals.

Keywords: entropy; time-frequency representation; electroencephalography; complexity

1. Introduction

Since the works of Kotelnikov and Shannon [1,2], it has been proved that the information provided by an event associated with the inverse of the probability of an event occurrence has been extremely useful for its significance and inherent conceptual simplicity.

The classical Shannon entropy measures the average information provided by a set of events and proves its uncertainty. This measure is shown as a natural candidate for quantifying the complexity of a signal. Also the level of chaoticity may be measured using entropy; therefore higher entropy represents higher uncertainty and a more irregular behavior of the signal. Moreover, if noise is added to an ordered signal the uncertainty increases and the entropy is also increased. Entropy can even explain how linked complex systems interact and exchange information. The quantification of the magnitude of this information becomes a goal in the study of biological signals.

The entropy estimation consists in calculating the probability of events that occur in time signals and in obtaining a reliable average value of the information provided by each of these events. The evolution of the entropy of a signal with respect to time, calculated from the instantaneous information of a window that slides over the signal, is a smoothing of the sequence of instantaneous information because the entropy is the average value of the information in this window.

The purpose of this paper is both to avoid this low-pass filtering inherent in the calculation of the entropy and to obtain instantaneous values of this measure. The time-frequency representation (TFR) technique is suited to achieve both aims. TFR generalizes the concept of the time and frequency domains to a joint time—frequency function that indicates how the frequency content of a signal changes over time [3,4]. Complexity studies based on entropy functional take advantage of the analogy between signal energy densities and probability densities [5]. While the instantaneous and spectral amplitudes behave as one-dimensional densities of signal energy in time and in frequency, TFR tries to act as 2-dimensional energy densities in both time and frequency [6].

In this paper, we investigate new measures that quantify the complexity and information content of a signal. Selecting time and frequency functions that satisfy marginal properties, one can assume that the energy density of a signal in one instant (or instantaneous power of the signal) is given by the entropy associated with the frequency components of the signal at this time instant (or instantaneous entropy). By similar reasoning, an equivalent measure can be obtained in the frequency domain (spectral information entropy). Thus, a different way to calculate the information in the TFR by estimating a probability density function of a signal either in time or in frequency domain is proposed in this paper. In a similar study, Baraniuk [6] discussed the calculation of the logarithms of Shannon expression with negative value of TFR. In this work this problems is avoided since the probability density of the TFR always contains positive values. Our proposed methodology is based on the original concept of

information defined as the logarithm of the inverse value of a probability. This permits to make a comparison with traditional Shannon entropy.

The Choi-Williams distribution (CWD) [3] is a type of Time-Frequency Representation (TFR) whose properties facilitate the purpose of this work. Four novel indexes are defined on the CWD: (1) partial instantaneous entropy, calculated as the entropy of the CWD with respect to time by using the probability mass function at each time instant taken independently; (2) partial spectral information entropy, calculated as the entropy of the CWD with respect to frequency by using the probability mass function of each frequency value taken independently; (3) complete instantaneous entropy, calculated as the entropy of the CWD with respect to time by using the probability mass function of the entire CWD; (4) complete spectral information entropy, calculated as the entropy of the CWD with respect to frequency by using the probability mass function of the entire CWD.

These indexes are tested on synthetic time series that simulate signals in which different behaviors (periodic, chaotic and random) are combined and on a dataset of electroencephalographic (EEG) signals recorded in different states (eyes-open, eyes-closed, ictal and non-ictal activity). For this analysis, EEG signals are selected since they are generated by nonlinear deterministic processes with nonlinear coupling interactions between neuronal populations [7].

2. Methodology

2.1. Time-Frequency Representation

CWD (1) is obtained by convoluting the Wigner distribution (WD) (2) and the Choi-Williams exponential (3) [3,8]:

$$CWD(t,f) = \iint_{-\infty}^{\infty} h(t-t', f-f')\, WDx\,(t', f')dt'df' \tag{1}$$

$$WDx(t,f) = \int_{-\infty}^{\infty} x(t+\tau/2)\; x^*(t-\tau/2)e^{-j2\pi f\tau}d\tau \tag{2}$$

$$h(t,f) = \sqrt{\frac{4\pi}{\sigma_c}}\, e^{-4\pi^2\frac{(tf)^2}{\sigma_c}} \tag{3}$$

The spectral power is defined as:

$$SpPow(f) = \int_{-\infty}^{\infty} CWD(t,f)\; dt \tag{4}$$

Choosing an adequate parameter σ_c, the function (3) is able to reduce WD cross-terms and preserve the properties of the WD, such as the marginal properties and instantaneous frequency. In this work, σ_c was set to 0.005 [8]. The $CWD(t,f)$ was normalized by the total power calculated as the area under *SpPow*.

2.2. Shannon Entropies

Entropy can express the mean of information that an event provides when it takes place, the uncertainty about the outcome of an event and the dispersion of the probabilities with which the events take place. Let X be a discrete random variable which takes a finite number of possible values $x_1, x_2, x_3..., x_n$ with probabilities $P(1), P(2), P(3)..., P(n)$ respectively, such that $P(i) \geq 0$, $i = 1, 2, 3...n$, $\sum_{i=1}^{n} P(i) = 1$; Shannon entropy (*Entr*) is defined as:

$$Entr = -\sum_{i=1}^{n} P(i) log_2\big(P(i)\big) \tag{5}$$

where n is the number of analyzed samples.

2.3. Instantaneous Entropy and Spectral Information Entropy

The probability mass function (PMF) was defined for a time instant t_k with respect to frequency as $pT_{PMF}(t_k, i) = P_{CWD}(CWD_i(t,f) \mid t = t_k)$ and for frequency value f_k with respect to time as $pF_{PMF}(i, f_k) = P_{CWD}(CWD_i(t,f) \mid f = f_k)$, after the quantization of the $CWD(t_k,f)$ and $CWD(t,f_k)$, respectively, in n=32 equidistant levels. In this work, a time range of $0 < t < 200$ s and a frequency bandwidth of $0 < f < 60$ Hz were taken into account.

The two distributions, quantization-time $pT_{PMF}(t, i)$ and quantization-frequency $pF_{PMF}(i, f)$, were obtained for each time instant and frequency value for the entire time $0 < t_k < 200$ s and bandwidth $0 < f_k < 60$ Hz. In this way, the two distributions represent partial distribution of PFM with respect to time or to frequency, since in each time instant (t_k) and frequency value (f_k) the PMF is only related to that time instant (t_k) or frequency value (f_k). In a similar way, the complete PMF distribution quantization-time and quantization-frequency were calculated as $cT_{PMF}(t, i) = P_{CWD}(CWD_i(t,f) \mid 0 < t < 200\ s)$ and $cF_{PMF}(i,f) = P_{CWD}(CWD_i(t,f) \mid 0 < f < 60\ Hz)$, respectively, after the quantization of the $CWD(t,f)$ in $n = 32$ equidistant levels.

From this proposed methodology, new indexes were defined:

- Partial instantaneous entropy:

$$pInstEntr(t) = -\sum_{i=1}^{n} pT_{PMF}(t,i) log_2\big(pT_{PMF}(t,i)\big) \tag{6}$$

- Partial spectral information entropy:

$$pSpInfEntr(f) = -\sum_{i=1}^{n} pF_{PMF}(i,f) log_2\big(pF_{PMF}(i,f)\big) \tag{7}$$

- Complete instantaneous entropy:

$$cInstEntr(t) = -\sum_{i=1}^{n} cT_{PMF}(t,i) log_2\big(cT_{PMF}(t,i)\big) \tag{8}$$

- Complete spectral information entropy:

$$cSpInfEntr(f) = -\sum_{i=1}^{n} cF_{PMF}(i,f) log_2\big(cF_{PMF}(i,f)\big) \tag{9}$$

3. Analyzed Data

3.1. Synthetic Signals

In order to study the performances of the *pInstEntr*, *pSpInfEntr*, c*InstEntr*, *cSpInfEntr* applied to different types of signals, a set of simulated signals were designed:

(1). A periodic signal $x(t) = \sum A_s \sin(2\pi F_i t)$ was generated adding a frequency component (F_i) every 25 s, in this way the first 25 s of the signal has 1 frequency component and the last 25 s has 8 frequency components. The added frequencies were respectively F_i = [0.5;1;2;5;10;20;30;50] Hz. The amplitude of each frequency component was $A_s = 1/N_F$, where $1 \leq N_F \leq 8$ is the number of the frequency components.

(2). A MIX process, used in previous studies [9–11], was defined as MIX = $(1 - z)x + zy$, where z is a random variable that is equal to 1 with probability p and equal to 0 with probability $1-p$, x is a periodic sequence with a frequency component of 10 Hz, and y is a standard uniformly distributed variable on $[-\sqrt{3},\sqrt{3}]$. The synthetic signal was based on a MIX process whose parameter p varied linearly from 0.9 to 0.1. Hence, this sequence, evolved from randomness to periodicity.

(3). The same MIX process of 2) using as y the Hx obtained from Henon map [12] with chaotic behavior (10), using the canonic values a = 1.4 and b = 0.3, and taking $Hx(0)$ = 0.5 and $Hy(0)$ = 0.5 as initial conditions. Hence, this sequence evolved from chaos to periodicity.

$$\begin{cases} Hx(n+1) = 1 - a\,Hx^2(n) + Hy(n) \\ Hy(n+1) = b\,Hx(n) \end{cases} \quad (10)$$

(4). The same MIX process of (3) using as y a Henon map with chaotic behavior and as x the standard uniformly distributed variable on $[-\sqrt{3},\sqrt{3}]$. Hence, this sequence evolved from chaos to randomness.

All synthetic signals had a length of 200 s and a sampling frequency of 128 Hz. For each synthetic signal, mean (m) of c*InstEntr, pInstEntr* and the signal entropy *Entr* were calculated with respect to time in windows of 1 s. The *cSpInfEntr* and *pSpInfEntr* and the spectral power of the CWD was also calculated for each signal.

3.2. Real EEG Recordings

A freely available EEG dataset was used for validation [13]. This dataset contains 100 single channel EEG segments of 23.6 s recorded with the same amplifier system, using an average common reference with a sampling rate of 173.6 Hz. The dataset was divided in five different sets (A, B, C, D, E). Sets A and B contain surface EEG signals recorded from five healthy volunteers who were relaxed in an awake state. Whereas the subjects had their eyes open during the recording of the EEG in set A, the EEG signals of dataset B were acquired with eyes closed. Three sets (C, D and E) of intracranial EEG recordings from five epileptic patients, who had achieved complete seizure control after a surgical procedure. Signals in set D were recorded within the epileptogenic zone, whereas the EEGs of set C were acquired from the opposite brain hemisphere. Sets C and D contained only activity measured during seizure-free intervals. On the other hand, set E was only composed of seizure activity recorded from all sites exhibiting ictal activity. Additional details can be found in [13].

4. Results and Discussion

4.1. Synthetic Signals

Figures 1–4 show the results obtained applying the methodology to all the synthetic signals.

Figure 1. Signal 1: (**a**) partial distribution quantization *vs*. time *pT*(*t*,*i*), (**b**) partial distribution quantization *vs*. frequency *pF*(*i*,*f*), (**c**) complete distribution quantization *vs*. time *cT*(*t*,*i*), (**d**) complete distribution quantization *vs*. frequency *cF*(*i*,*f*), (**e**) instantaneous complete entropy (*cInstEntr*), partial entropy (*pInstEntr*) and traditional entropy (*Entr*), (**f**) spectral complete information entropy (*cSpInfEntr*), partial information entropy (*pSpInfEntr*) and spectral power (*SpPow*).

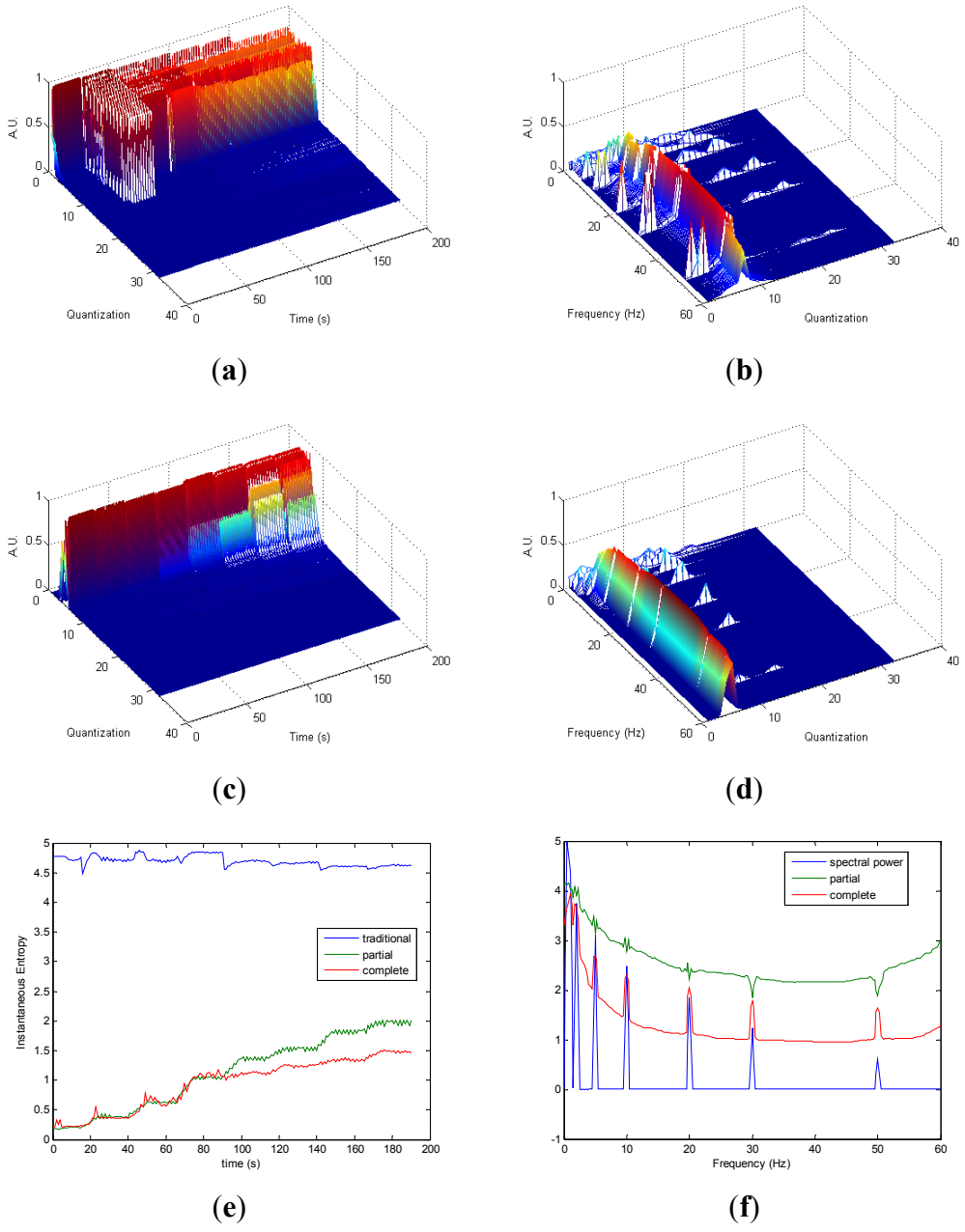

(**a**) (**b**)

(**c**) (**d**)

(**e**) (**f**)

Figure 2. Signal 2: (**a**) partial distribution quantization *vs*. time *pT*(*t*,*i*), (**b**) partial distribution quantization *vs*. frequency *pF*(*i*,*f*), (**c**) complete distribution quantization *vs*. time *cT*(*t*,*i*), (**d**) complete distribution quantization *vs*. frequency *cF*(*i*,*f*), (**e**) instantaneous complete entropy (*cInstEntr*), partial entropy (*pInstEntr*) and traditional entropy (*Entr*), (**f**) spectral complete information entropy (*cSpInfEntr*),partial information entropy (*pSpInfEntr*) and spectral power.

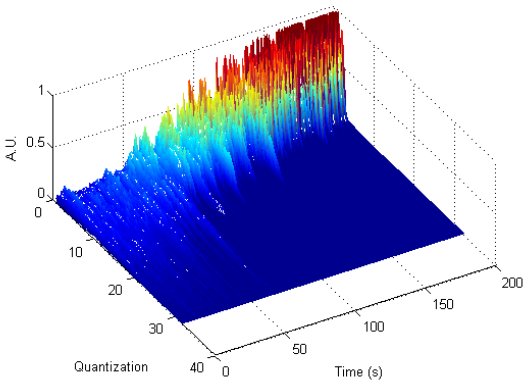

(a)

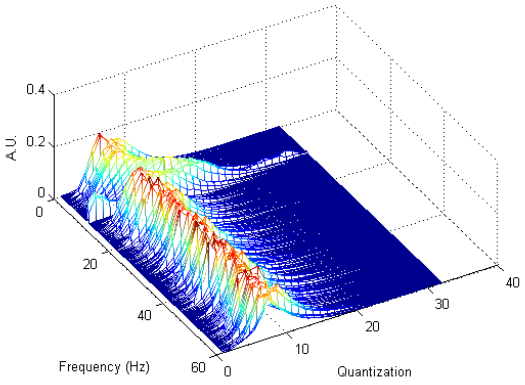

(b)

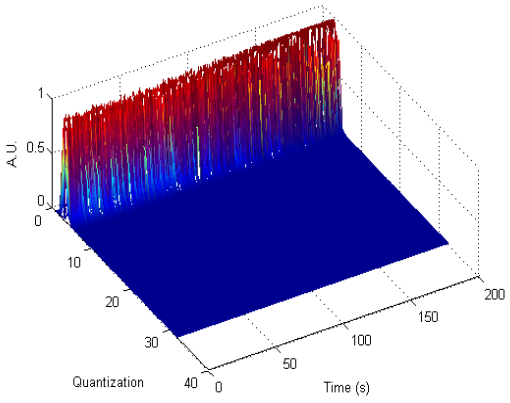

(c)

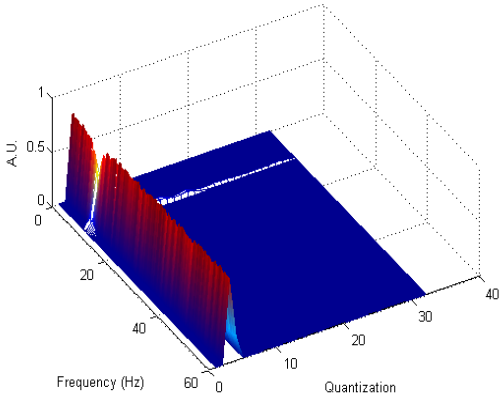

(d)

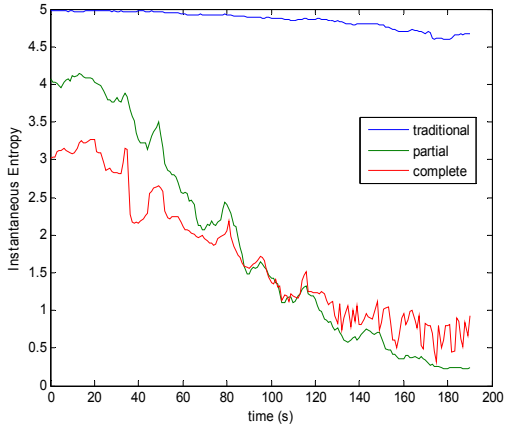

(e)

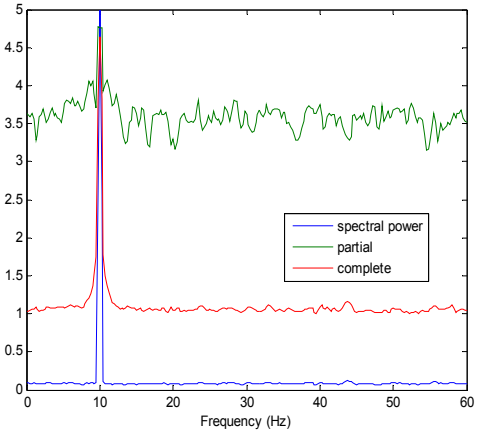

(f)

Figure 3. Signal 3: (**a**) partial distribution quantization *vs*. time *pT*(*t*,*i*), (**b**) partial distribution quantization *vs*. frequency *pF*(*i*,*f*), (**c**) complete distribution quantization *vs*. time *cT*(*t*,*i*), (**d**) complete distribution quantization *vs*. frequency *cF*(*i*,*f*), (**e**) instantaneous complete entropy (*cInstEntr*), partial entropy (*pInstEntr*) and traditional entropy (*Entr*), (**f**) spectral complete information entropy (*cSpInfEntr*),partial information entropy (*pSpInfEntr*) and spectral power.

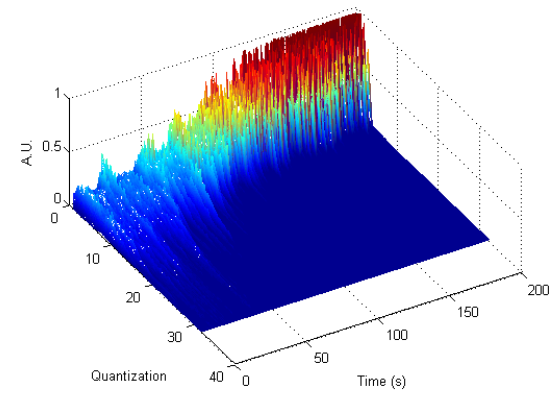

(**a**)

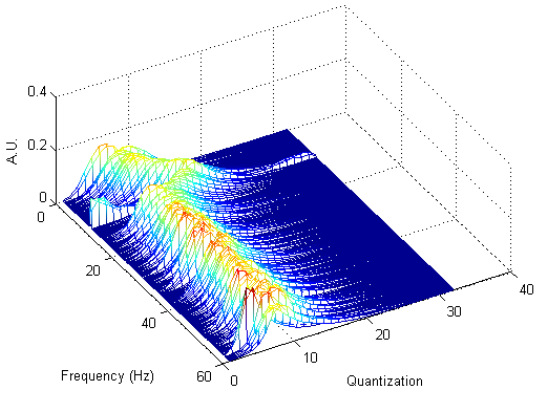

(**b**)

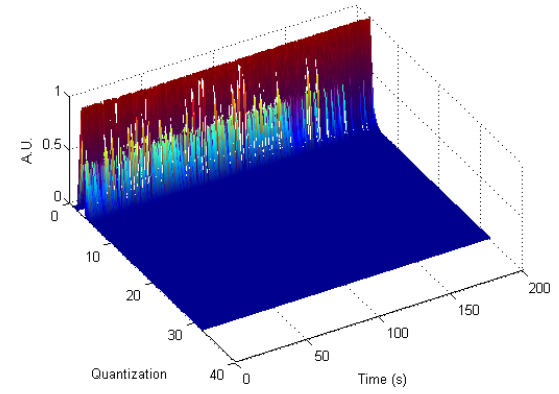

(**c**)

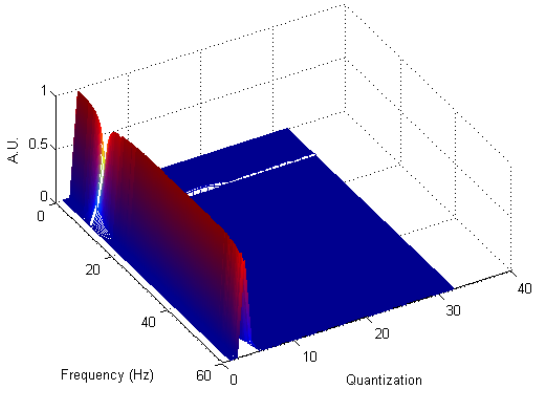

(**d**)

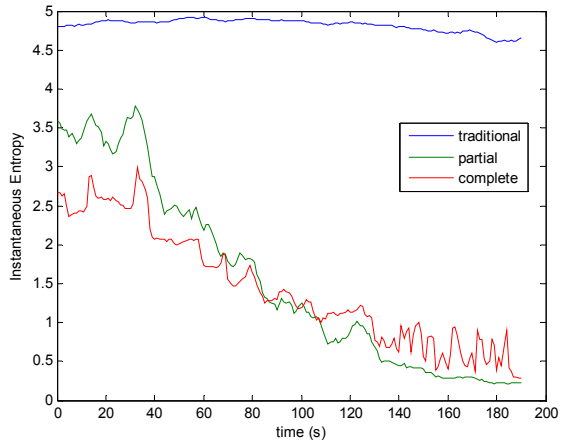

(**e**)

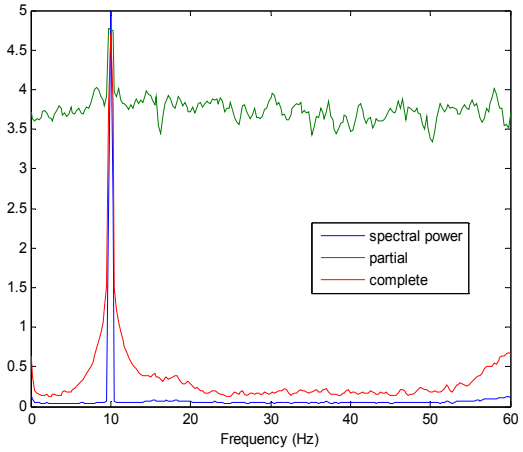

(**f**)

Figure 4. Signal 4: (**a**) partial distribution quantization *vs*. time *pT*(*t*,*i*), (**b**) partial distribution quantization *vs*. frequency *pF*(*i*,*f*), (**c**) complete distribution quantization *vs*. time *cT*(*t*,*i*), (**d**) complete distribution quantization *vs*. frequency *cF*(*i*,*f*), (**e**) instantaneous complete entropy (*cInstEntr*), partial entropy (*pInstEntr*) and traditional entropy (*Entr*), (**f**) spectral complete information entropy (*cSpInfEntr*), partial information entropy (*pSpInfEntr*) and spectral power.

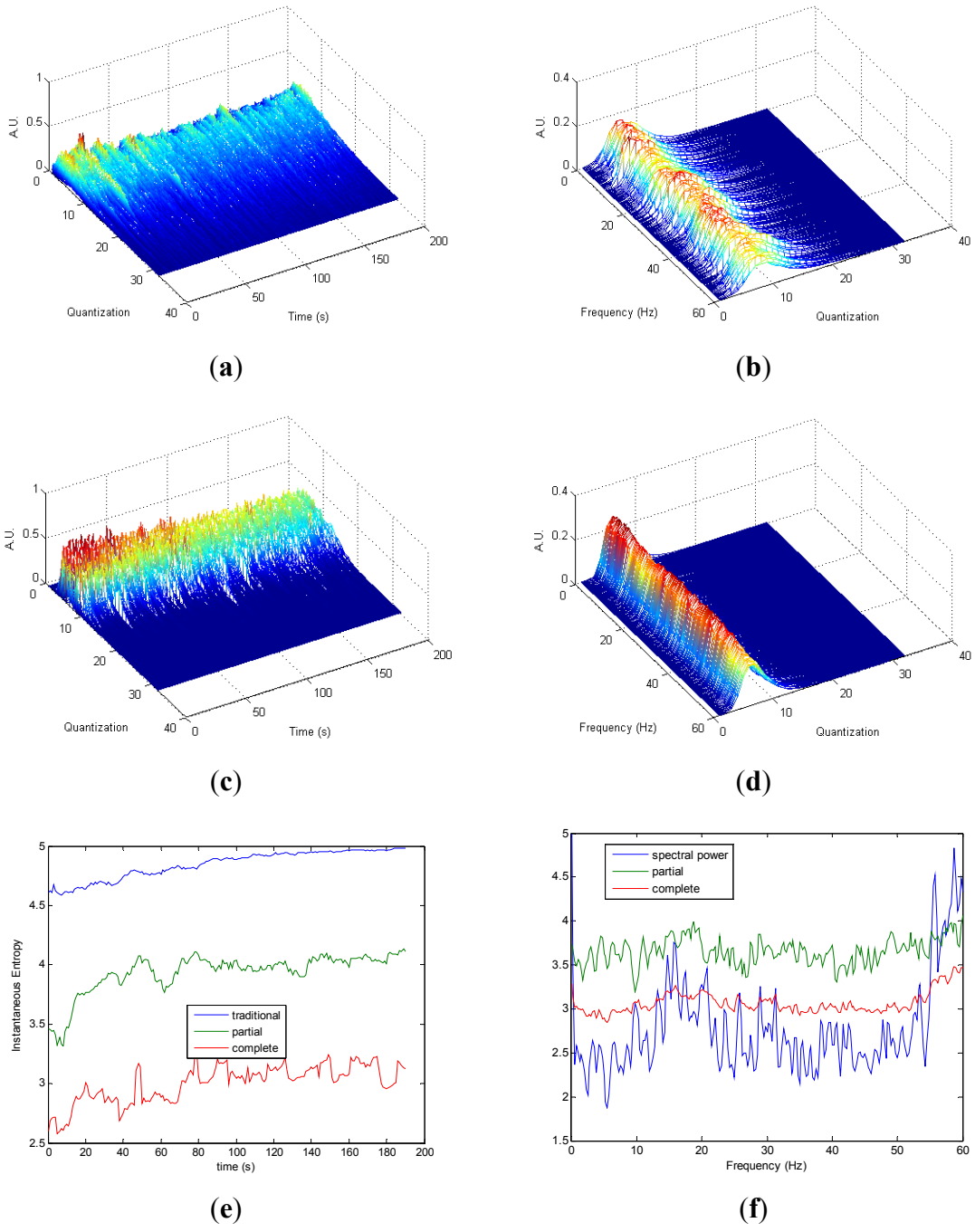

(**a**) (**b**) (**c**) (**d**) (**e**) (**f**)

Partial and complete distribution quantization *vs*. time of signal 1 are presented in Figures 1a,c, respectively. It can be observed that in *cT* all information is contained in few quantization bins, due to the fact that the quantization takes into account the complete CWD. On the contrary, since the quantization of *pT* takes into account separately the values of each time instant of CWD, the distribution

of quantization-time is more homogeneous. Similar behavior is followed by *pF* and *cF*, as it is shown in Figures 1b,d, respectively. As it can be noted in Figure 1e, traditional *Entr* does not show significant changes when signal 1 evolves from one frequency component to the eight simultaneous frequency components, while $pInstEntr$ and $cInstEntr$ increase from one frequency component to the multiple components. However, $pInstEntr$ has a higher increase than $cInstEntr$. In the frequency domain (Figure 1f), $pSpInfEntr$ and $cSpInfEntr$ have similar behavior to $SpPow$, showing the location of the frequency components $f = F_i$. However $pSpInfEntr$ and $cSpInfEntr$ decrease in low frequency until about 20 Hz and then they maintain stable values for $f \neq F_i$. The higher values of $pSpInfEntr$ and $cSpInfEntr$ at low frequencies correspond to the persistent frequency components along the signal 1. The values of $pSpInfEntr$ are above $cSpInfEntr$ and approximately equidistant for all frequency values, except for the high frequency components (f = 30 Hz and f = 50 Hz) where $pSpInfEntr$ and $cSpInfEntr$ assume similar values.

Partial and complete distributions quantization *vs*. time of signal 2 are presented in Figures 2a,c. During the transition from randomness to periodicity, the evolution of *pT* (Figure 2a) presents some changes that are less evident in *cT* (Figure 2c). The evolution of *pT* tends to be homogenous in the zone with more randomness. Observing quantization-frequency distributions in Figures 2b,d, all information is more contained in few quantization bins in *cF* than *pF*, due to the fact that the quantization takes into account the complete CWD in *cF*. In both *pF* and *cF* distributions, the oscillation frequency of the sinusoid is observed in 10 Hz. Traditional *Entr* (Figure 2e) does not show significant changes when the signal passes from a random to a periodic behavior. On the contrary, $pInstEntr$ and $cInstEntr$ decrease from randomness to periodicity. During random behavior $pInstEntr$ is higher than $cInstEntr$, then the two measures approach each other and converge in the zone with more periodicity. In Figure 2f, $pSpInfEntr$ and $cSpInfEntr$ show the location of the frequency component as $SpPow$ does. While $cSpInfEntr$ maintains stable values for the remaining frequencies, $pSpInfEntr$ presents irregular oscillations in the entire spectrum. Values of $pSpInfEntr$ are higher than $cSpInfEntr$ except for the frequency component of the signal f = 10 Hz.

Similarly to the evolutions observed in Figure 2a,c, it can be noted in Figure 3a,c that the differences in the transition from chaos to periodicity in the evolution of *pT* (Figure 3a) are less evident in *cT* (Figure 2c). It is observed that less homogeneity behavior is preserved in *pT* in the zone with more chaos (Figure 3a) compared to the zone with more random (Figure 2a). Also, it can be noted that *cT* presents more heterogeneity along the time than in Figure 2c, due to the differences between chaos and random series. Quantization-frequency distributions of signal 3 (Figures 3b,d) have similar behavior to signal 2 (Figure 2b,d). Also *Entr*, $pInstEntr$, $cInstEntr$ (Figure 3e), $pSpInfEntr$ and $cSpInfEntr$ (Figure 3f) exhibit similar behavior to signal 2. However, it can be noted when Figures 2f and 3f are compared that $cSpInfEntr$ has a higher and a more constant base-line for all frequencies in signal 2 (Figure 2f) than in signal 3.

Quantization-time distributions of signal 4 are shown in Figure 4a,c. Certain differences are observed in the transition from chaos to randomness in the evolution of both *pT* and *cT*. The behavior of both distributions appear to be homogeneous. As it was observed in signals 1, 2 and 3, the information contained in quantization-frequency distributions of signal 4 (Figure 4b,d) is more concentrated in *cF* than *pF*. Then, since the complete distribution appears to be always more concentrated in few bins, it can be used when more resolution is required. Observing Figure 4e, *Entr*, $pInstEntr$ and $cInstEntr$

increase their values from chaos to random behavior of the signal. The entropy $pInstEntr$ has higher values than $cInstEntr$ for all the time instants. As it can be observed in Figure 4f, *SpPow*, $pSpInfEntr$ and $cSpInfEntr$ have similar behavior showing oscillations around three different constant baselines. Higher values are observed in $pSpInfEntr$ than in $cSpInfEntr$.

Comparing the Figures 1e, 2e, 3e, and 4e, it can be deduced that when the signals contain many different frequency components, $pInstEntr$ is higher than $cInstEntr$. This behavior is observed from approximately $t = 100$ s in Figure 1e, and till $t = 60$ s in Figures 2e and 3e. This is corroborated in Figure 4e where the analyzed signal combines chaos and random features along the time. However, when the signals have few frequency components, $pInstEntr$ and $cInstEntr$ have similar values. Comparing Figures 1f, 2f, 3f, and 4f, it is observed that both $pSpInfEntr$ and $cSpInfEntr$ tend to assume the same value where a frequency peak is present in the spectrum. For the remaining frequency components, $pSpInfEntr$ has always higher values than $cSpInfEntr$.

4.2. Real EEG Signals

Figures 5–9 show the averaged evolution of c*InstEntr*, *pInstEntr, Entr*, *cSpInfEntr*,*pSpInfEntr* and $SpPow$ of all EEG signals of each set. It can be observed that entropy *pInstEntr* has higher values than c*InstEntr* in set A and B for all time instants (Figures 5a and 6a, respectively), however, different behavior is seen in sets C, D and E (Figures 7a, 8a and 9a, respectively) where few slightly differences are observed between these two indexes. Traditional entropy *Entr* is always the highest. Observing Figures 5b, 6b, 7b, 8b and 9b, it can be noted that *pSpInfEntr* presents almost constant shape with higher values than *cSpInfEntr* for the entire frequency spectrum. On the contrary, the shape of *cSpInfEntr* is similar to $SpPow$, both presenting peaks in correspondence to certain frequency values. Entropies *pSpInfEntr* and *cSpInfEntr* tend to increase in high frequencies while the $SpPow$ is zero.

Figure 5. Set A (awake state with eyes open): (**a**) instantaneous complete entropy (*cInstEntr*), partial entropy (*pInstEntr*) and traditional entropy (*Entr*), (**b**) spectral complete information entropy (*cSpInfEntr*), partial information entropy (*pSpInfEntr*) and spectral power.

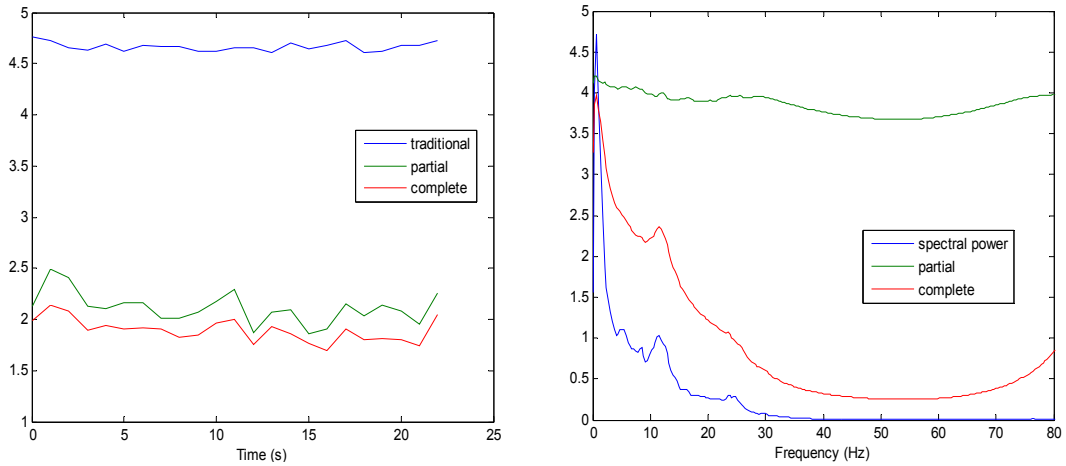

(**a**) (**b**)

Figure 6. Set B (awake state with eyes closed): (**a**) instantaneous complete entropy (*cInstEntr*), partial entropy (*pInstEntr*) and traditional entropy (*Entr*), (**b**) spectral complete information entropy (*cSpInfEntr*), partial information entropy (*pSpInfEntr*) and spectral power.

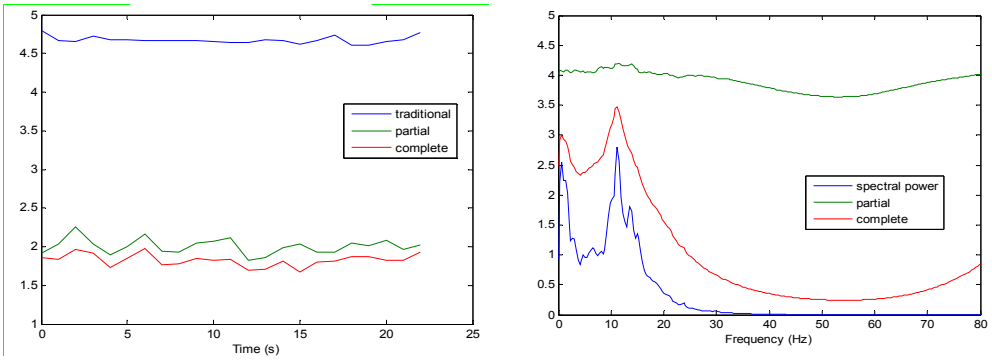

(**a**) (**b**)

Figure 7. Set C (non-ictal activity recorded from the epilogenetic zone): (**a**) instantaneous complete entropy (*cInstEntr*), partial entropy (*pInstEntr*) and traditional entropy (*Entr*), (**b**) spectral complete information entropy (*cSpInfEntr*), partial information entropy (*pSpInfEntr*) and spectral power.

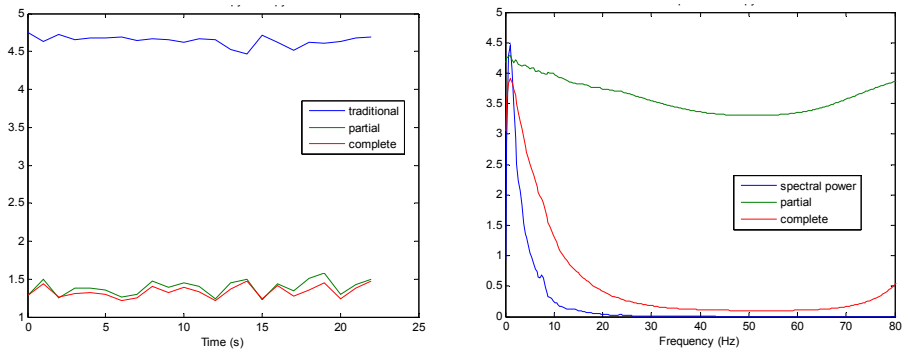

(**a**) (**b**)

Figure 8. Set D (non-ictal activity recorded from opposed brain hemisphere to set C): **(a)** instantaneous complete entropy (*cInstEntr*),partial entropy (*pInstEntr*) and traditional entropy (*Entr*), **(b)** spectral complete information entropy (*cSpInfEntr*), partial information entropy (*pSpInfEntr*) and spectral power.

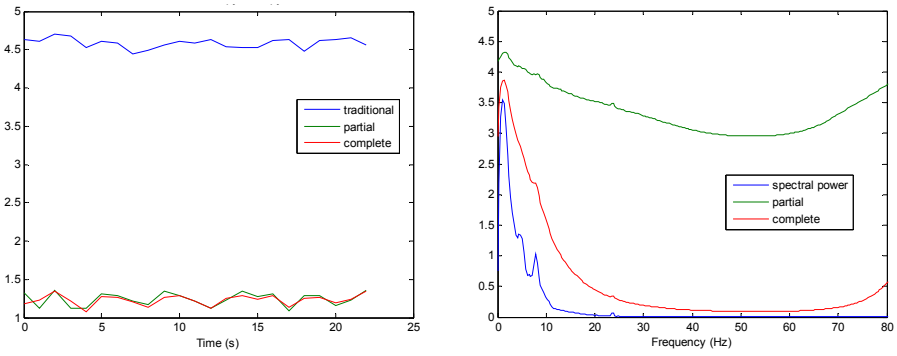

(**a**) (**b**)

Figure 9. Set E (ictal activity): (**a**) instantaneous complete entropy (*cInstEntr*), partial entropy (*pInstEntr*) and traditional entropy (*Entr*), (**b**) spectral complete information entropy (*cSpInfEntr*), partial information entropy (*pSpInfEntr*) and spectral power.

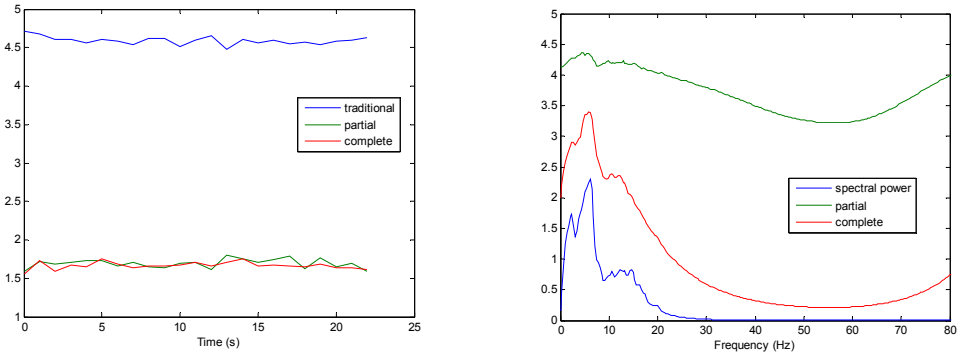

(**a**) (**b**)

Figure 10 shows the boxplot of the mean values of *pInstEntr*, *pSpInfEntr*, c*InstEntr*, *cSpInfEntr* and *Entr* calculated for each EEG signal of each set (A,B,C,D,E). Table 1 contains the *p*-values (Mann-Whitney U-test) of the analyzed measures obtained by comparing sets: A *vs*. B, C *vs*. D, C *vs*. E and D *vs*. E.

The fundamental assumption of nonlinear techniques is that EEG signal is generated by nonlinear deterministic processes with nonlinear coupling interactions between neuronal populations. Nonlinearity in the brain is introduced, even at the neuronal level [13]. In recent years, with the application of the nonlinear dynamics to EEG, more evidences have indicated that the brain is a nonlinear dynamic system, and EEG signal can be regarded as its output [14]. In this way, it has been assumed that EEG signal is between random signal and deterministic signal [15].

As it can be seen in Figures 10c,d, higher values of c*InstEntr* and *cSpInfEntr* are related to eyes-closed state (set B) compared to eyes-open state (set A), with *p*-value = 0.0059 and *p*-value < 0.0005 (Table 1), respectively. Therefore, it can be inferred that the closing of eyes is associated with higher entropy in time and in frequency. Comparing these values with the evolution of the synthetic signals, higher entropy in time domain (c*InstEntr*) is associated with a predominance of random behavior respect to chaotic behavior and periodicity. Related to *cSpInfEntr*, the higher values of set B indicate a much more complexity behavior than in set A. It can be observed that *cSpInfEntr* of a random signal mixed with periodicity components (Figure 2f) contains a constant baseline with values higher than a chaotic signal mixed with periodicity components (Figure 3f). Therefore, it might be assumed that a random signal mixed with periodicity components has higher mean value of *cSpInfEntr* than a chaotic signal mixed with periodicity components. Then, *cSpInfEntr* of set A seems to have a behavior similar to chaos mixed with periodicity (shown in Figure 3f) and *cSpInfEntr* of set B seems to have a behavior similar to random mixed with periodicity (shown in Figure 2f).

Regarding the sets C, D and E of the EEG database, there are very significant differences between the values of *pInstEntr*, *pSpInfEntr*, c*InstEntr*, *cSpInfEntr* computed for non-ictal (sets C and D) and ictal (set E) states, with *p*-value < 0.0005 (Table 1). In this case, the higher value of these measures in ictal activity is associated with more complex behavior in time-frequency domain. Since the literature [16] is almost concordance to the fact that epileptic seizure is associated with a decrease of complexity of the

EEG signal in time domain, we assume that higher values of *pInstEntr, pSpInfEntr, cInstEntr, cSpInfEntr* in set E seem to indicate a higher complexity in frequency domain.

Figure 10. EEG signals: (**a**) partial instantaneous entropy (*pInstEntr*), (**b**) partial spectral information entropy (*pSpInfEntr*), (**c**) complete instantaneous entropy (*cInstEntr*), (**d**) complete spectral information entropy (*cSpInfEntr*), (**e**) traditional entropy (*Entr*). set A: awake state with eyes open; set B: awake state with eyes closed; set C: non-ictal activity recorded from the epilogenetic zone; set D: non-ictal activity recorded from opposed brain hemisphere to set C; set E: ictal activity. On each box, the central mark is the median, the edges of the box are the 25th and 75th percentiles. The whiskers are lines extending from each end of the boxes to show the extent of the rest of the data. Values beyond the end of the whiskers are considered outliers and marked with a +.

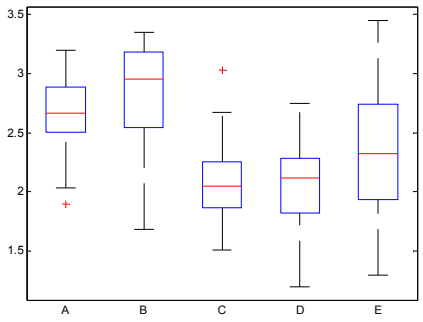

(**a**)

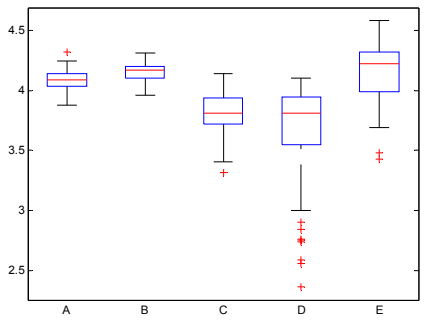

(**b**)

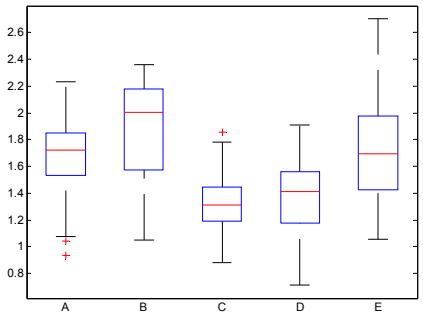

(**c**)

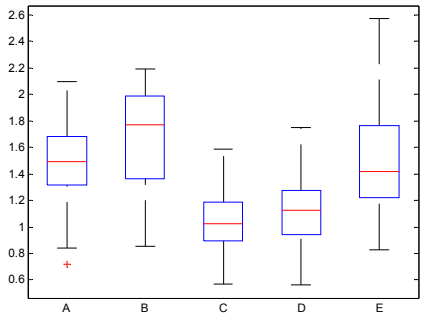

(**d**)

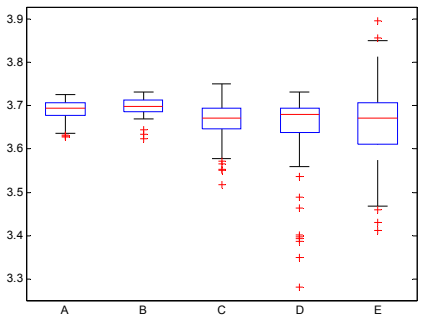

(**e**)

Table 1. EEG signals: *p*-values of the entropy measures obtained by comparing sets.

Sets	*pInstEntr*	*pSpInfEntr*	*cInstEntr*	*cSpInfEntr*
A *vs*. B	0.2360[n.s.]	0.1547 [n.s.]	0.0059	0.00003
C *vs*. D	0.9861[n.s.]	0.0147	0.1096[n.s.]	0.0399
C *vs*. E	<0.0005	<0.0005	<0.0005	<0.0005
D *vs*. E	<0.0005	<0.0005	<0.0005	<0.0005

n.s., non-statistical significant.

Certain differences are observed between the inter-ictal activity recorded from the epilogenetic zone (set C) and from the opposite brain hemisphere (set D) in the frequency domain (*pSpInfEntr* and *cSpInfEntr* in Figures 10(b,d), respectively), with p-value < 0.05. However, there are not statistical differences between the inter-ictal activity recorded from the epilogenetic zone (set C) and from the opposite brain hemisphere (set D) in the time domain (*pInstEntr* and c*InstEntr* in Figures 10(a,c), respectively).

Figure 11. EEG signals: (**a**) partial instantaneous entropy (*pInstEntr*) in alpha band (**b**) partial instantaneous entropy (*pInstEntr*) in beta band, (**c**) complete instantaneous entropy (*cInstEntr*) in delta band (**d**) complete instantaneous entropy (*cInstEntr*) in alpha band. Set A: awake state with eyes open; set B: awake state with eyes closed; set C: non-ictal activity recorded from the epilogenetic zone; set D: non-ictal activity recorded from opposed brain hemisphere to set C; set E: ictal activity. On each box, the central mark is the median, the edges of the box are the 25th and 75th percentiles. The whiskers are lines extending from each end of the boxes to show the extent of the rest of the data. Values beyond the end of the whiskers are considered outliers and marked with a +.

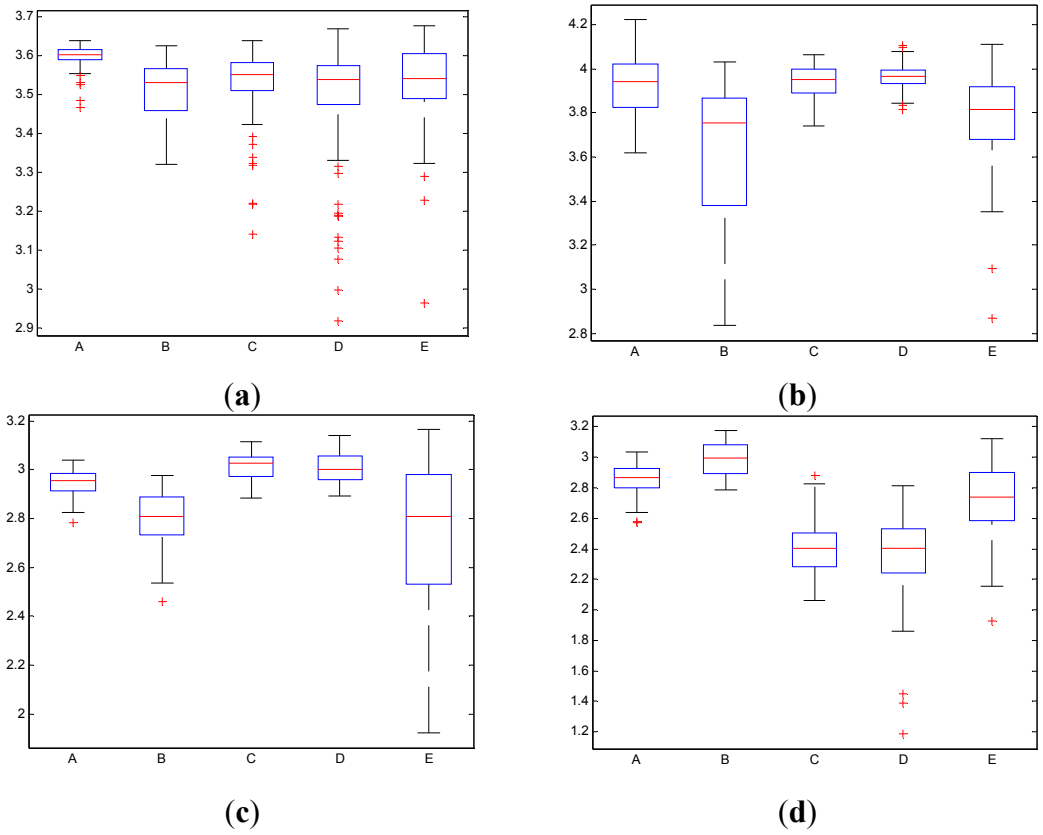

In contrast to the traditional time domain information measures as the *Entr*, the CWD permits to divide the spectrum in order to isolate specific frequency bands. This property permits to calculate the *pInstEntr*, *pSpInfEntr*, c*InstEntr*, *cSpInfEntr* in the traditional frequency bands of the EEG signal (delta, theta, alpha, beta, gamma). Figures 11 and 12 show the boxplot of the distributions of the *pInstEntr*, *pSpInfEntr*, c*InstEntr*, *cSpInfEntr* calculated in the frequency bands that give the best statistical significant results. The statistical significance levels are presented in Table 2.

Figure 12. EEG signals: (**a**) partial spectral information entropy (*pSpInfEntr*) in beta band, (**b**) complete spectral information entropy (*cSpInfEntr*) in beta band. Set A: awake state with eyes open; set B: awake state with eyes closed; set C: non-ictal activity recorded from the epilogenetic zone; set D: non-ictal activity recorded from opposed brain hemisphere to set C; set E: ictal activity. On each box, the central mark is the median, the edges of the box are the 25th and 75th percentiles. The whiskers are lines extending from each end of the boxes to show the extent of the rest of the data. Values beyond the end of the whiskers are considered outliers and marked with a +.

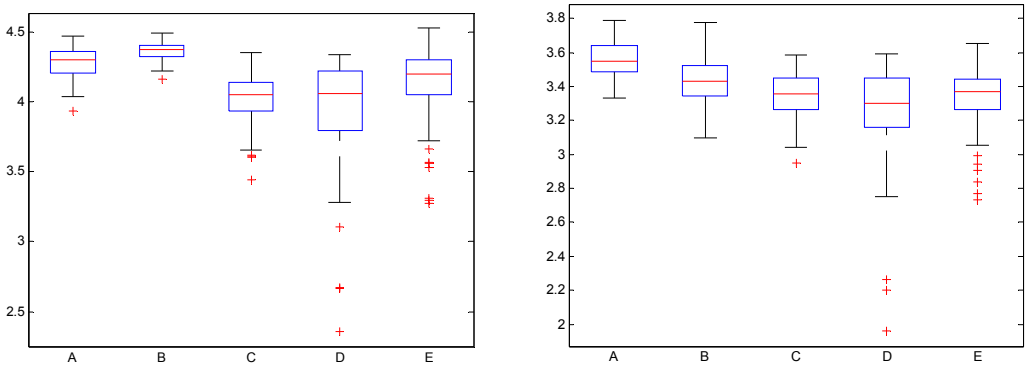

(**a**) (**b**)

Table 2. EEG signals: *p*-values of the entropy measures obtained by comparing sets.

Sets	***pInstEntr***		***cInstEntr***		***pSpInfEntr***	***cSpInfEntr***
	alfa band	**beta band**	**delta band**	**alfa band**	**beta band**	**beta band**
A *vs*. B	<0.0005	<0.0005	<0.0005	<0.0005	<0.0005	<0.0005
C *vs*. D	0.0706$^{n.s.}$	0.0467	0.2328$^{n.s.}$	0.9013$^{n.s.}$	0.8214$^{n.s.}$	0.0235
C *vs*. E	0.9151$^{n.s.}$	<0.0005	<0.0005	<0.0005	<0.0005	0.9249$^{n.s.}$
D *vs*. E	0.1284$^{n.s.}$	<0.0005	<0.0005	<0.0005	<0.0005	0.0341

n.s., non-statistical significant.

It is well known that the closed eyes condition produces certain changes in the EEG. One of the most remarkable alterations is the rise in the power of the alpha rhythm [13]. Thus, the EEG spectrum is modified in comparison to the eyes-open case. These modifications have been also detected by the instantaneous and spectral information entropy measures depicted in Figures 11 and 12.

As it can be seen in Figure 11a–c, lower values of *pInstEntr* in alpha and beta, and *cInstEntr* in delta are related to the eyes-closed state (set B) compared to eyes-open state (set A), with p-value < 0.0005. On the contrary, *cInstEntr* assumes higher values in set B than set A with p-value < 0.0005 when alpha band is studied. Therefore, it can be inferred that the closing of eyes causes

transference of information between delta and alpha frequency bands. In addition, the boxplots depicted in Figure 11a,d show differences between sets A and B, *pInstEntr* values decrease from set A to set B while *cInstEntr* values increase. Since the value obtained considering independently each time instant (partial distribution *pT*) has different behavior from the value obtained considering all time instants (total distribution *cT*) we assume that the information provided by the alpha rhythm presents non-stationary behavior. Regarding the subsets C, D and E of the EEG database, there are very significant differences between non-ictal (sets C and D) and ictal (set E) states, due to the values of *pInstEntr* in beta (Figure 11b), c*InstEntr* in delta (Figure 11c) and in alpha frequency bands (Figure 11d), with p-value < 0.0005. In this case, higher values of *pInstEntr* in beta (Figure 11b) and in delta band (Figure 11c) are observed in non-ictal activity (sets C and D) while c*InstEntr* has a reverse behavior (Figure 11d).

Higher values of *pSpInfEntr* in beta band (Figure 12a) are related to the eyes-closed state (set B) compared to eyes-open state (set A), with p-value < 0.0005. Contrarily, *cSpInfEntr* (Figure 12(b)) assumes lower values in set B than in set A with p-value < 0.0005 when beta band is studied. This behavior indicates a high contain of power in beta band for eyes-open state (set A) compared with eyes-closed state (set B), as it is observed in *cSpInfEntr* (Figure 12b). Contrarily, high values of *pSpInfEntr* in eyes-closed state indicate that the beta rhythm is more regularly present along the time of the EEG recording. These different behaviors are observed in synthetic signal 1 in which the low frequencies are present in all the evolution of the simulated signal (Figure 1f). Regarding the subsets C, D and E of the EEG database, there are very significant differences (p-value < 0.0005) between non-ictal (sets C and D) versus ictal (set E) states, however only for the values of *pSpInfEntr* in beta band (Figure 12a). In this case, higher values of *pSpInfEntr* in beta (Figure 12a) are observed in ictal activity (set E).

Table 3 shows the sensitivity (*Sen*) and specificity (*Spe*) calculated with the leaving-one-out method and the area under the ROC curve (*AUC*) of the best measures obtained by comparing EEG sets. It can be noted that measures of *pInstEntr*, *cInstEntr* and *SpInfEntr* permitted to obtain *Sen* > 65%, *Spe* > 70% and *AUC* > 0.75 in the discrimination between A and B sets. Furthermore, measures of *pInstEntr* and *cInstEntr* yield *Sen* > 75%, *Spe* > 80% and *AUC* > 0.8 in the discrimination between C, D and E sets.

Table 3. EEG signals: sensitivity (*Sen*), specificity (*Spe*) and area under ROC curve (*AUC*) of the best entropy measures obtained by comparing sets.

Sets	***Measure***	***Sen***	***Spe***	***AUC***
A *vs*. B	*pInstEntr (alfa)*	69.0	90.3	0.896
	cInstEntr (delta)	67.6	90.3	0.905
	cSpInfEntr(beta)	66.2	72.2	0.784
C *vs*. E	*cInstEntr*	76.8	82.8	0.881
	cInstEntr (alfa)	77.8	82.8	0.874
	cInstEntr (beta)	73.7	63.6	0.758
D *vs*. E	*cInstEntr*	83.8	75.8	0.893
	pInstEntr (beta)	61.6	96.0	0.853

5. Conclusions

A new approach to calculate TFR entropy has been presented and applied to simulated and real physiological time series. This approach is based on the definition of Shannon entropy applied to the

probability mass function of the TFR in both time and frequency domain. In this way, the smoothing inherent in the calculation of the entropy is avoided and instantaneous values of this measure are obtained.

This methodology takes advantage of the property inherent to TFR that permits to deal with non-stationary signals together with the property of Shannon entropy that deals with chaoticity, complexity and randomness.

The results have shown that the values of the proposed measures tend to decrease, with different proportion, when the behaviors of the synthetic signals evolve from chaos or randomness to periodicity. Finally, this paper has demonstrated that they can be useful tools to quantify the different periodic, chaotic and random components in EEG signals.

Acknowledgments

This work was supported within the framework of the CICYT grant TEC2010-20886 from the Spanish Government and the Research Fellowship Grant FPU AP2009-0858 from the Spanish Government. CIBER of Bioengineering, Biomaterials and Nanomedicine is an initiative of ISCIII.

Author Contributions

All authors collaborated and contributed extensively to the work presented in this paper. More specifically: Umberto Melia, Francesc Claria and Montserrat Vallverdu designed the methodology and wrote the paper; Umberto Melia carried out the development of the algorithms and the application of the entropy measures to real and simulated signals; Pere Caminal had the general overview of the work.

Conflicts of interest

The authors have declared no conflicts of interest.

References

1. Kotelnikov, V.A. On the carrying capacity of the ether and wire in telecommunications. In Proceedoings of the First All-Union Conference on Questions of Communication, Izd. Red. Upr. Svyazi RKKA, Moscow, Russia, 1933.
2. Shannon, C.E. Communication in the presence of noise. *Proc. Inst. Radio Eng.* **1949**, *37*, 10–21; Reprint in: *Proc. IEEE* **1998**, *86*, 2.
3. Cohen, L. *Time-Frequency Analysis*; Prentice Hall Signal Processing Series; Prentice Hall: Englewood Cliffs, NJ, USA, 1995.
4. Flandrin, P. *Time-Frequency and Time-Scale Analysis*; Academic: San Diego, CA, USA, 1999.
5. Williams, W.J.; Brown, M.L.; Hero, A.O. Uncertainty, information, and time-frequency distributions. *Proc. SPIE Int. Soc. Opt. Eng.* **1991**, *1566*, 144–156.
6. Baraniuk, R.G. Measuring Time–frequency information content using the Rényi entropies. *IEEE Trans. Inf. Theor.* **2001**, *47*, 1391–1409.
7. Jeong, J. EEG dynamics in patients with Alzheimer's disease. *Clin. Neurophysiol.* **2004**, *115*, 1490–1505.

8. Clariá, F.; Vallverdú, M.; Riba, J.; Romero, S.; Barbanoj, M.J.; Caminal, P. Characterization of the cerebral activity by timefrequency representation of evoked EEG potentials. *Physiol. Meas.* **2011**, *32*, 1327–1346.
9. Pincus, S.M. Approximate entropy as a measure of system complexity. *Proc. Natl. Acad. Sci. USA* **1991**, *88*, 2297–2301.
10. Ferrario, M.; Signorini, M.G.; Magines, G.; Cerutti, S. Comparison of entropy-based regularity estimators: Application to the fetal heart rate signal for the identification of fetal distress. *IEEE Trans. Biomed. Eng.* **2006**, *53*, 119–125.
11. Escudero, J.; Hornero, R.; Abasolo, D. Interpretation of the auto-mutual information rate of decrease in the context of biomedical signal analysis. Application to electroencephalogram recordings. *Physiol. Meas.* **2009**, *30*, 187–199.
12. Davies, B. *Exploring Chaos theory And Experiment*; Perseus Books: Reading, MA, USA, 1999.
13. Andrzejak, R.G.; Lehnertz, K.; Moormann, F.; Rieke, C.; David, P.; Elger, C.E. Indications of nonlinear deterministic and finite-dimensional structures in time series of brain electrical activity: Dependence on recording region and brain state. *Phys. Rev.* **2001**, *64*, 061907.
14. Korn, H.; Faure, P. Is there chaos in the brain? II. Experimental evidence and related models. *Comptes Rendus Biol.* **2003**, *326*, 787–840.
15. Wang, X.; Meng, J.; Tan, G.; Zou, L. Research on the relation of EEG signal chaos characteristics with high-level intelligence activity of human brain. *Nonlinear Biomed. Phys.* **2010**, *4*, 2.
16. Babloyantz, A.; Destexhe, A. Low-dimensional chaos in an instance of epilepsy. *Proc. Natl. Acad. Sci. USA* **1986**, *83*, 3513–3517.